The Detection of Shaft Misalignments using Motor Current Signals from a Sensorless Variable Speed Drive

Samieh Abusaad[1], Ahmed Benghozzi[1], Ann Smith[1], Fengshou Gu[1], Andrew Ball[1]

[1]Centre for Efficiency and Performance Engineering, University of Huddersfield, Huddersfield, U.K.

E-mail: f.gu@hud.ac.uk

Abstract Shaft misalignments are common problems in rotating machines which cause additional dynamic and static loads, and vibrations in the system, leading to early damages and energy loss. It has been shown previously that it is possible to use motor current signature analysis to detect and diagnose this fault in motor drives. However, with a variable speed drive (VSD) system, it becomes difficult to detect faults as the drive compensates for the small changes from fault effects and increased noise in the measured data. In this paper, motor current signatures including dynamic and static data have been investigated for misalignment diagnosis in a VSD system. The study has made a systemic comparison of different control parameters between two common operation modes: open loop and sensorless control. Results show that fault detection features on the motor current from the sensorless mode can be the same as those of the open loop mode, however, the detection and diagnosis is significantly more difficult. In contrast, because of the additional frictional load, features from static data show results of early detection and diagnosis of different degrees of misalignment is as good as that from conventional vibration methods.

Key words: Sensorless VSD, Misalignment, Current Signature, Condition Monitoring, Vibration.

1.0 Introduction

Shaft misalignments give rise to major problems in rotating machines which often cause additional dynamic loads and vibrations in the system, leading to early damages and energy loss. Studies show that badly aligned machines can cost a factory 20% to 30% of machines downtime [1]. Other studies show that misalignment is the source of 70% of vibration problems [2]. Moreover, it also consumes additional energy [3]. Many studies have been made using different diagnosis and detection techniques for early and effective monitoring of shaft misalignments. For in-

stance vibration [4-5], wireless sensors [6-7], model based fault diagnosis [8-9], and motor current signature analysis [10-11]. However, most of these studies were performed on motors fed through either direct mains or V/Hz drives.
Previous studies on the detection of faults in a mechanical system driven by a sensorless VSD have been limited. One of the main reasons for this is that the drive's control system compensates for any dynamic effects caused by the fault and introduces more noise to the measured data. Therefore, frequency components commonly used could be masked by the drive actions. In addition, the harmonic contents at the terminal output parameters from the drive, and in particular the stator current and voltage, is high, which makes it more difficult to identify the small changes in current signatures [12-13].
In this study, motor current signature analyses have been conducted to study the behaviour of current signals under two control modes: V/Hz open loop and sensorless mode are subject to parallel misalignments occurring with different degrees of severity in a gearbox test system. Both instantaneous or dynamic current signals from an external sensor and average or static current data from the drive are examined to benchmark the performance of these two data sources.

2.0 Sensorless VSD

Sensorless flux vector control drives are very common nowadays in industry due to their improved dynamic performance, accurate speed control, higher efficiency, lower operating cost and higher reliability. Sensorless VSDs represent three phase AC motor currents in a single phase d-q reference frame. Both d and q current components are regulated separately copying the way the DC machines work. The flux is regulated by controlling the d current component while the torque is regulated by adjusting the q current component. The motor speed is estimated and compared with the speed set point in order to generate the reference voltage to the pulse width modulator which sets the duty cycles for the inverter. Figure 1 represents the general structure of sensorless VSDs. However, when the system operates at or higher than the rated speed, the output voltage must be limited to the DC-Bus voltage of the drive and the output current is saturated to the rated motor current.
In general, mechanical faults such as misaligned shafts will cause the load torque of the motor to oscillate at a frequency relating to the mechanical faults. This torque oscillation will lead to speed oscillation. To minimize this speed oscillation the VSD drive will adjust i_q to react against any speed changes. The drive therefore will continually adjust the terminal supply to maintain the system in stable conditions. As shown in [14], this type of fault can be identified by inspecting the spectral peaks at frequencies that are related to the rotor mechanical speed in the motor current spectrum at the following frequencies:

$$f_x = f_s \pm k f_r \qquad k = 1,2,3,\ldots \tag{1}$$

Where: f_x the feature fault frequency component, f_s supply frequency, f_r rotor mechanical frequency. In addition to the dynamic oscillations, the misalignment will also cause additional static friction. As reported in [15] there will be up to 1.2% energy loss due to the frictional loss caused by misalignment, which will require an increase in electrical torque and hence an increase in current and voltage to overcome the additional load and maintain the operation at setpoints. Therefore it is also possible to detect misalignment by the static current values.

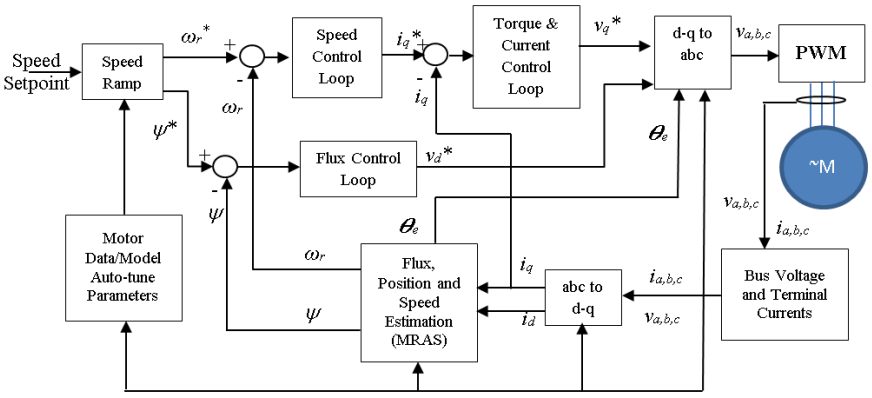

Fig. 1 General structure of sensorless VSD**.**

Where: ω_r rotor angular speed, d-q refers to the direct and quadrature axis respectively in the d-q plane, i_d and v_d current and voltage field components respectively, i_q and v_q current and voltage torque components respectively, ψ flux linkage, $i_{a,b,c}$ and $v_{a,b,c}$ the three phase line currents and voltages respectively, θ_e supply phase angle, MRAS model reference adaptive system estimator, the subscript * refers to the reference values, and PWM the pulse width modulator in the VSD.

3.0 Test Facility

The system employed for this study consists of two main parts: the mechanical part and the control part, as shown in Figure 2. The mechanical part consists of one 15kW AC induction motor as the prime driver, two back-to-back 2 stage helical gearboxes for coupling the DC motor with the AC motor, flexible spider couplings link the components. The first gearbox operates as a speed reducer while the second is a speed increaser so that the system maintains sufficient speed for the DC motor to generate sufficient load to the AC motor. The control system consists of a programmable logic controller (PLC) for setting up test profiles requested by the operator, an AC VSD that can be set either to sensorless flux vector control or V/Hz modes for adjusting the speed of the system, a DC variable speed

drive providing a controlled load to the AC motor by regulating the torque of the DC motor/generator.
In addition, a low speed data log system is employed to log the static data from the VSD at the rate of 1Hz. In the meantime a high speed data acquisition system operates at 96kHz to log dynamic data from the system, which includes three accelerometers attached to the two gearboxes and the AC IM for monitoring the vibration levels; one shaft encoder attached to the AC motor. Three terminals measure voltage and current using Hall Effect sensors. The accelerometers are placed horizontally in parallel with shafts centerlines, as shown in Figure 2. All data sets from the data acquisition systems are stored in a PC for post processing and analysis in the Matlab environment. This dynamic data is for both the evaluation of the performance of conventional analysis methods and the benchmark of the performance developed from static data.

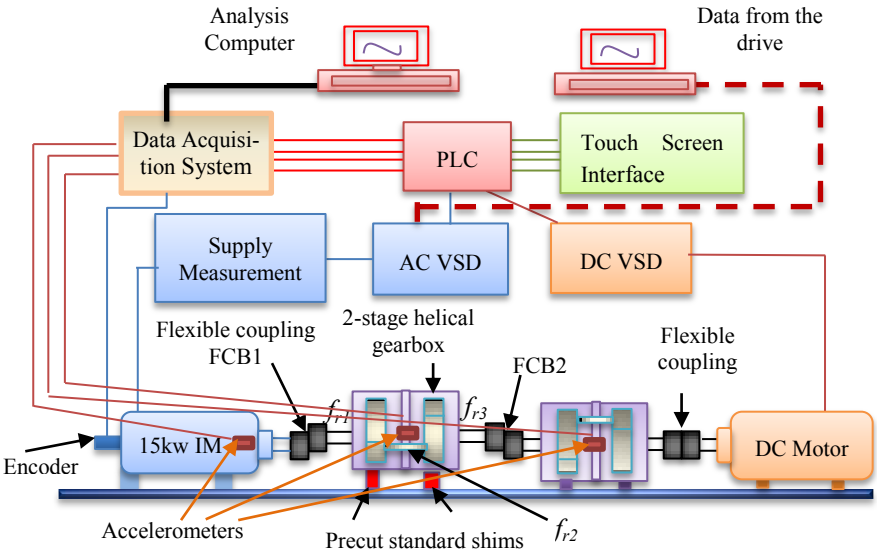

Fig. 2 Schematic represents the test rig layout and fault induced.

Four different degrees of severities of shaft misalignment are simulated at 0.5 mm, 0.7mm, 1.00 mm and 1.30 mm successively which are induced by raising up the gearbox next to the AC motor using precut stainless steel standard shims placed under the gearbox as indicated in Figure 2. The test rig is firstly aligned at the lowest possible vibration level. A cycle of 5 different load settings was applied, 0%, 25%, 50%, 75% and 100% of the full load. Each load applied for a period of two minutes. The AC motor speed is set at its full speed during the tests. A set of 10 seconds of dynamic data is collected for each load, while the data from the VSD is collected for the entire cycle.

Figure 3 shows the vibration signals from gearbox 1 under different misalignment severities and loads. It can be seen that the vibration amplitudes at 3X of f_{r1} and of f_{r3} increasing consistently with the degrees of the misalignment, showing that the fault cases are induced appropriately. Therefore, these results can be a benchmark of the current signals analysis and diagnosis method developed in this paper.

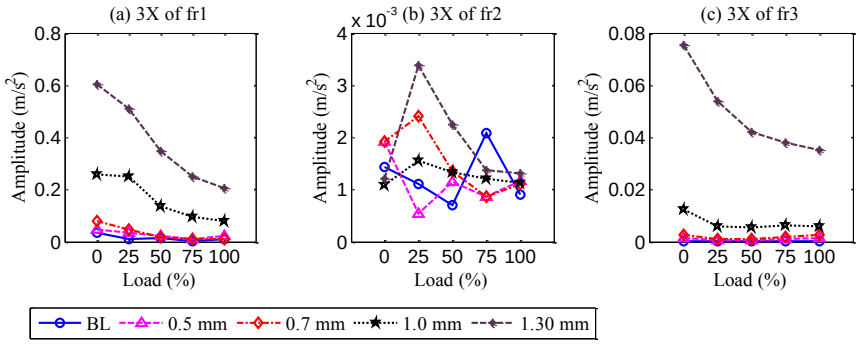

Fig. 3 Vibration signals comparison at 3X of f_{r1} and of f_{r3} under different severities.

4.0 Results and Analysis

To investigate the performance of the current signals in differentiating the misalignment, the dynamic current signals are converted into the frequency domain and the amplitudes extracted and compared at corresponding feature frequencies: *fr1* and *fr3*. Meanwhile a direct comparison of the static current signals is made between the baseline and different misalignment cases to examine their detection performance in line with the results from the dynamic data and vibration signals.

4.1 Detection and Diagnosis under Open Loop

To show the general characteristic, Figure 4 shows a comparison of current spectrum between 1.0 mm misalignment and the baseline under 50% and 100% load. It can be seen that the components at f_{r3} are distinctive and the 3X components are higher than the first and the second, showing the basic feature of the three jaw coupling. Moreover, the amplitude at f_{r3} sidebands increases with the degree of misalignment, which is consistent with fault severities. However, the amplitude decreases with load due to the effect of the nonlinear behavior of the coupling.
Components at f_{r1} increase with the misalignment but the amplitudes are not clearly identifiable due to high background noise from the VSD. The component at 1x

of f_{r2} shows a little change with fault severity as the shaft is the internal one of the gearbox.

To diagnose the fault severity, sideband components at the 3X f_{r1} and f_{r3} are extracted and presented against loads in Figure 5 Figure 5(a) shows the misalignment on the first shaft is just detectable by the current spectrum at the high severity of 1.3mm. Meanwhile the misalignment on the third shaft can be detected and quantified starting from 0.7mm, as shown in Figure 5(b). The reason for higher sensitivity to the third shaft is that it undertakes a torsional load 3.6 times of the first shaft.

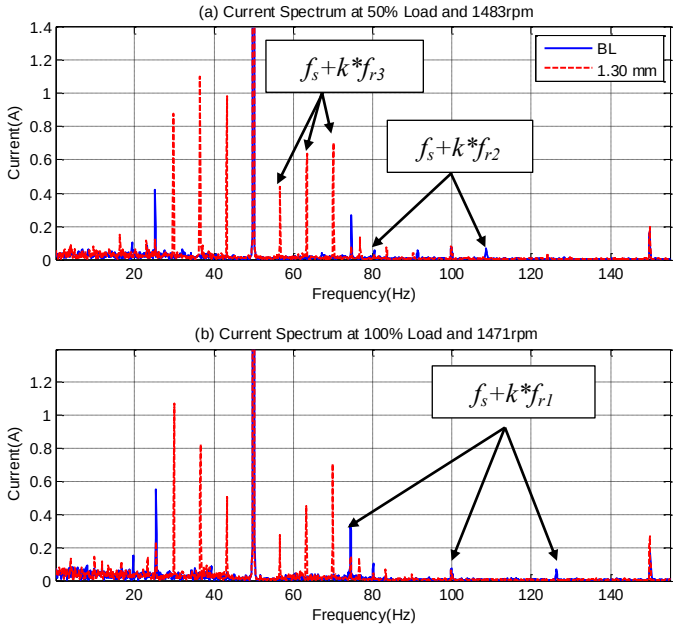

Fig. 4 Current spectra under different load and cases

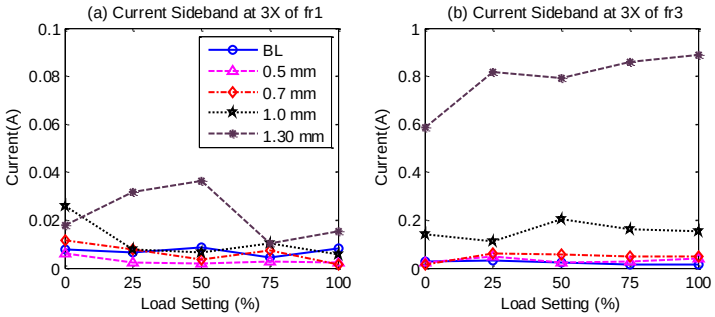

Fig. 5 Current 3X of $f_{r1}$and f_{r3} comparison under different misalignments and loads.

Under open-loop mode, there is no speed feedback to the drive. Instead the drive provides a constant *V/Hz* ratio. In the case of the misalignment, there is early indication that additional fractional torque is induced. This friction adds additional static load on the motor which in turn causes an additional electromagnetic torque and more current in the motor. Consequently, static torque and current signals are most likely to be affected by such faults. Figure 6 represents the average of current, torque, i_d and i_q signals under different load and misalignment conditions. Both the torque and torque current component i_q show a gradual increase with an increase in misalignment levels. So they can be used for fault classification. Nevertheless, the field current component i_d has no clear change related to the fault severity. Authors reported in [16] a new cos effective technique utilising data from sensorless VSDs for mechanical misalignment detection. Noticeably even when the misalignment is as small as 0.5mm it can be clearly detected from both torque and i_q signals. This shows that the static data has a better sensitivity than that of the dynamic data under the open loop operation.

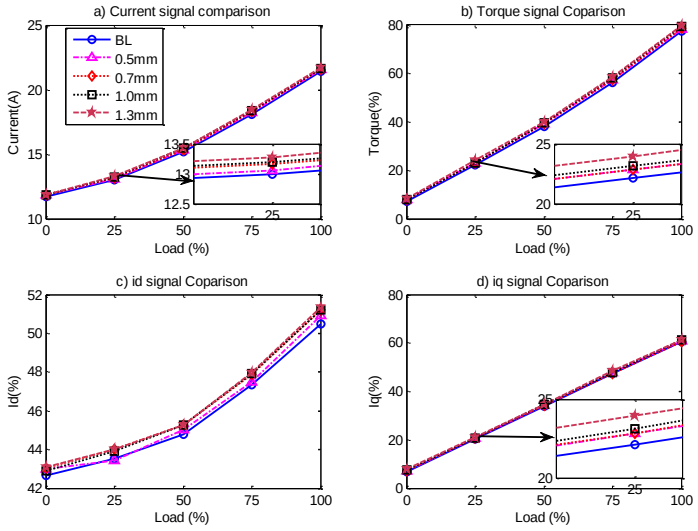

Fig. 6 Current, torque, i_q and i_d comparison at different fault severities and loads.

4.2 Detection and Diagnosis under Sensorless Mode

In sensorless control mode, the drive adjusts the motor supply parameters keeping the speed of the machine stable and follows the reference without feedback encoder. When a fault occurs due to an abnormality such as misalignment, it changes the stability conditions. The drive's regulators will adjust the machine's supply to compensate for the effects of defects on the load and speed. As a consequence of

this control processes and that of the level of noise from the IGBs on the PWM which is very high, the sideband frequency components of current signal cannot be easily observed. As depicted in Figure 7 (a), rotor frequency f_{r1} of the current spectrum and its sidebands do not show any clear changes correlated with the fault severities.

On the other hand, the components at 3X of f_{r3} show identifiable changes at 1.0 and 1.30 mm, as detailed in Figure 7 (b). However, severities at and below the 0.7 mm are difficult to discriminate. This shows that it is less possible to detect and diagnose the small faults under the sensorless mode, compared with that of open loop mode.

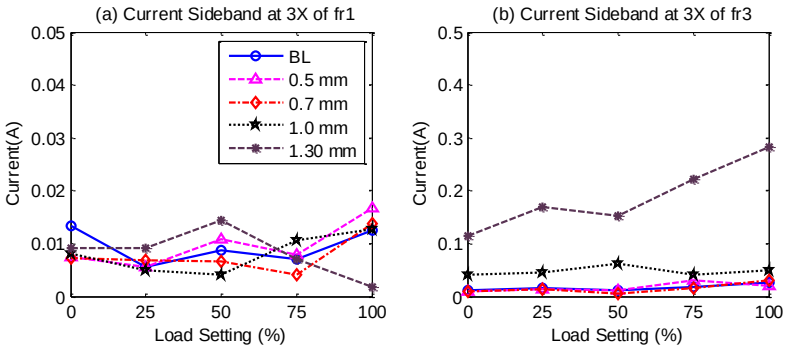

Fig. 7 Current sidebands 3x of f_{r1} and f_{r3} with different fault and load conditions

Data from the drive was acquired at the same time as the dynamic data was collected under the sensorless operation. Figure 8 shows the system variables under different degrees of severity and loads. It shows that current, i_q components and torque signals vary with the fault severity. This is due to the fact that the motor needs more torque to recover from the disturbances from the misalignment. This shows that misalignment has induced a static load in addition to the dynamic oscillations. Conversely, i_d is changing slightly, but not correlating with the fault severity. In order to maintain the speed at the desired value the drive feeds more current compensating for any disturbances due to misalignment. Therefore most torque related signals have been changing with the fault severity. Authors reported in [16] a new cost effective technique utilising static data for detecting mechanical misalignment in systems driven by sensorless VSDs. Polynomial models have been developed and trained for baseline conditions. In cases of abnormalities, it generates residuals related to the fault severities.

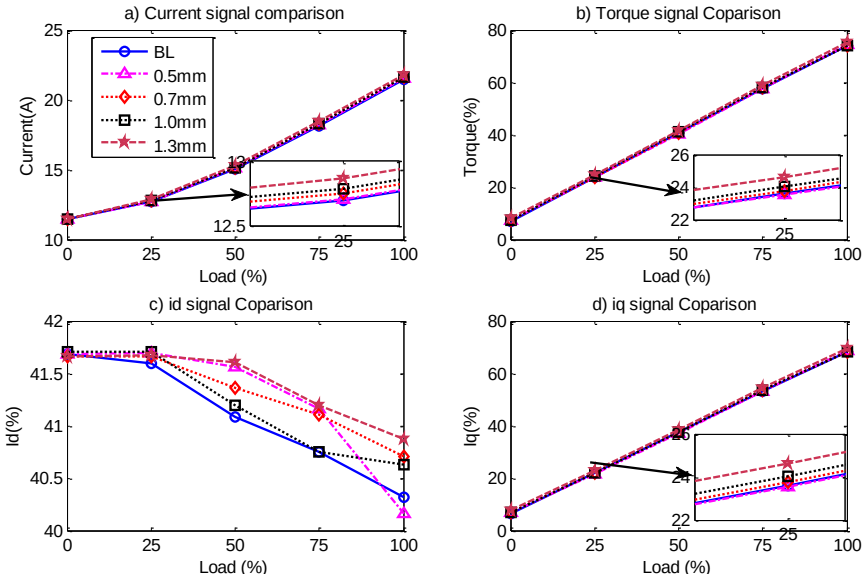

Fig. 8. Data from Sensorless VSD comparison under different misalignment severities and loads

5.0 Conclusion

The study shows that motor current data can be used for shaft misalignment detection under sensorless operation. The detection features from dynamic data are consistent with those of open-loop, i.e. the sidebands around the supply frequency due to the effect of load and speed oscillation. However, the detection performance is lower than that of open loop operation because of the effect of oscillation compensation and noise contamination from the drive.

On the other hand the misalignment creates additional frictional loads to the systems which need more electrical power to overcome it. Based on this understanding, the static data from the drive under both the open and sensorless operations can be used to detect and diagnose all different levels of misalignments. In particular, the torque related variables such as i_q current and torque signals show consistent changes correlated with the degree of severities. This has demonstrated that this static based misalignment detection outperforms that of the dynamic data and shows the same performances as that of conventional vibration analysis.

References

[1] Ahmed, M., Ahmed, K., Imran1, M. Shuja. Khan, Akram1, T., Jawad1, M. 2010. Spectral analysis of misalignment in machines using sideband components of broken rotor bar, Shorted Turns and Eccentricity. International Journal of Electrical & Computer Sciences IJECS-IJENS, Vol.10, No. 6, 2010.

[2] Bognatz S. R, 1995. Alignment of critical and non-critical machines. Orbit 23–25.

[3] Howard A. G. and Ray C., 1999. Energy Losses caused by Machinery misalignment and unbalance.17th International model analysis conference-IMAC XVII 1999.

[4] Tejas H, and AshishK D., 2009. Experimental investigations on vibration response of misaligned rotors. Mechanical Systems and Signal Processing, 23(7), pp.2236–52

[5] Nagrani, S., Pathan, S., and Bhoraniya, I. 2012. Misalignment fault diagnosis in rotating machinery through the signal processing technique- signature analysis, International Journal of Advanced Engineering Research and Studies E-ISSN2249–8974, (2012).

[6] Arebi, L., Gu F., and Ball, A. 2012. A comparative study of misalignment detection using a novel Wireless Sensor with conventional Wired Sensors, 25th International Congress on Condition Monitoring and Diagnostic Engineering, (2012).

[7] Arebi, L., Gu F., Hu, N. and Ball, A. 2011. Misalignment detection using a wireless sensor mounted on a rotating shaft, 24th International Congress on Condition Monitoring and Diagnostics Engineering Management. COMADEM, Stavanger, Norway, pp. 1289-1299. (2011).

[8] Jalan, Kr., and Mohanty, A.R., 2009. Model based fault diagnosis of a rotor–bearing system for misalignment and unbalance under steady-state condition. Journal of Sound and Vibration, Vol. 327, pp.604-622

[9] Tichate W., Poj T., Cherdchai P., Mongkol P. 2006. Motor Misalignment Detection Based on Hidden Markov Model. Structural Health Monitoring. Vol. 6, pp. 325-334.

[10] Blodt, M., Chabert, M., Regnier, J., Faucher, J., Dagues, B. 2005. Detection of mechanical load faults in induction motors at variable speed using stator current time-frequency analysis. Diagnostics for Electric Machines, Power Electronics and Drives, 2005. SDEMPED 2005. 5th IEEE International Symposium 2005, pp.1-6.

[11] Obaid, R. R., Habetler, T. G, and Tallam, R. M. 2003. Detecting load unbalance and shaft misalignment using stator current in inverter-driven induction motors. IEEE International Electric Machines and Drives Conference (IEMDC'03), Vol. 3, USA, 2003, pp.1454-1458.

[12] Bellini, A., Filippetti, F., Franceschini, G. and Tassoni, C. (2000) 'Closed-Loop Control Impact on the Diagnosis of Induction Motors Faults' IEEE Trans. on Ind. Applications. Vol. 36, pp.1318-1329.

[13] Kolodziejek, P., and Elzbieta, B. (2009) 'Broken rotor bar impact on Sensorless control of induction machine'. The International Journal for Computation and Mathematics in Electrical and Electronic Engineering. Vol. 28. pp. 540 – 555

[14] Schoen, R. R. and Habetler, T. G. 1995. Effects of time-varying loads on rotor fault detection in induction machines. IEEE Trans. Ind. Appl., Vol. 31, pp. 900–906.

[15] Howard A. G. and Ray C., 1999. Energy Losses caused by Machinery misalignment and unbalance.17th International model analysis conference-IMAC XVII 1999.

[16] Abusaad, S., Benghozzi, A., Shao, Y., Gu, Fengshou and Ball, A., 2013. Utilizing Data from a Sensorless AC Variable Speed Drive for Detecting Mechanical Misalignments. Key Engineering Materials, 569. pp. 465-472. ISSN 1013-9826.